Advances in Concrete Construction, *Vol. 9, No. 2* (*2020*) *115-123*
DOI: https://doi.org/10.12989/acc.2020.9.2.115

Role of fibers on the performance of geopolymer concrete exterior beam column joints

S. Deepa Raj*[1], N. Ganesan[2a] and Ruby Abraham[3b]

[1]*Department of Civil Engineering, College of Engineering Trivandrum, Kerala, India*
[2]*Department of Civil Engineering, National Institute of Technology Calicut, Kozhikode, Kerala, India*
[3]*Marian Engineering College, Kerala, India*

(*Received January 13, 2019, Revised November 10, 2019, Accepted November 26, 2019*)

Abstract. The performance of steel fiber reinforced geopolymer concrete beam column joints under cyclic loading was investigated. The volume fraction of fibers considered were 0.25% (19.62 kg/m^3), 0.5% (39.24 kg/m^3), 0.75% (58.86 kg/m^3) and 1% (78.48 kg/m^3). A total of fifteen specimens were prepared and tested under reverse cyclic loading. Test results were analyzed with respect to first crack load, ultimate load, energy absorption capacity, energy dissipation capacity, stiffness degradation and load deflection behavior. Test results revealed that the addition of steel fibers enhanced the performance of geopolymer concrete beam column joints significantly. The joints were analyzed using finite element software ANSYS. The analytical results were found to compare satisfactorily with the experimental values.

Keywords: geopolymer concrete; steel fiber; beam column joint; ductility; stiffness degradation; energy dissipation

1. Introduction

The main ingredient of conventional concrete is Ordinary Portland cement (OPC). Cement industry is responsible for 5 to 7 % of total global carbon dioxide emission (CO_2) to the atmosphere (Shaikh 2014). Use of geopolymer as an alternative concrete binder has revolutionized the concept of concrete design all around the world. Davidovits initiated the industrial research in geopolymer in 1972, aimed to develop alternate binder for concrete. Fly ash is the foremost source material for geopolymer since it is abundantly available in many parts of the world and it contains amorphous alumina silica (Hardjito *et al*. 2004, Jindal 2018, Shaikh 2014). Recent research studies revealed that geopolymer concrete has properties favorable for potential use as a construction material. It has high compressive strength, little drying shrinkage, low creep and good resistance to acid and sulfate attacks (Rangan 2006, Ganesan *et al*. 2015, Shaikh 2014, Kurtoglu *et al*. 2018). A few studies have been reported on the use of such GPCs for structural applications. The structural behavior of geopolymer concrete columns subjected to axial compressive loading and uniaxial bending were studied by various researchers (Sujatha *et al*. 2012, Sarker 2009) and found that GPC columns exhibited higher load carrying capacity and less deformation than corresponding RCC columns. The studies on geopolymer concrete beams revealed that the performance of GPC beams were superior to conventional concrete beams of the same grade (Dattreya *et al*. 2011).

Beam-column joints in a reinforced concrete moment resisting frames are crucial zones for transfer of loads effectively between the connecting elements in the structure. When forces larger than the design force are developed during earthquakes, joints get severely damaged (Ganesan *et al*. 2014, Lee *et al.* 2009). The magnitude of horizontal and vertical shear forces in beam-column joint region is several times greater than that developed in adjacent beams and columns when it is subjected severe seismic excitations Fiber reinforced concrete resist more cycles of loading even after cracking. The important seismic characteristics such as toughness, energy dissipation capacity and damage tolerance of concrete have improved by the addition of fibers (Ganesan *et al*. 2014, 2015). The addition fibres significantly improved the engineering properties such split tensile strength, modulus of elasticity and poisons ratio of geopolymer concrete (Ganesan *et al*. 2013). The experimental investigations on the structural behavior of conventional concrete beam column joints showed that the strength of joint depends on several factors such as reinforcement detailing, bond strength, amount of lateral ties, dimensions of beam and column, strength of concrete, column axial load, percentage of fibers etc. (Haach *et al*. 2008, Wing *et al.* 2012). Even though large number of studies has been conducted to understand the mechanical properties of GPC, studies on structural behavior of GPC are limited and studies on geopolymer concrete beam column joints are very limited. This study is an extension of previous work reported by the same authors in 2015 and 2016, they reported that the performance of geopolyemer concrete beam column joints

∗Corresponding author, Associate Professor
E-mail: deeparaj@cet.ac.in
[a]Ph.D.
E-mail: nganesan@nitc.ac.in
[b]Ph.D.
E-mail: rubyraju@yahoo.co.in

ISSN: 2287-5301 (Print), 2287-531X (Online)

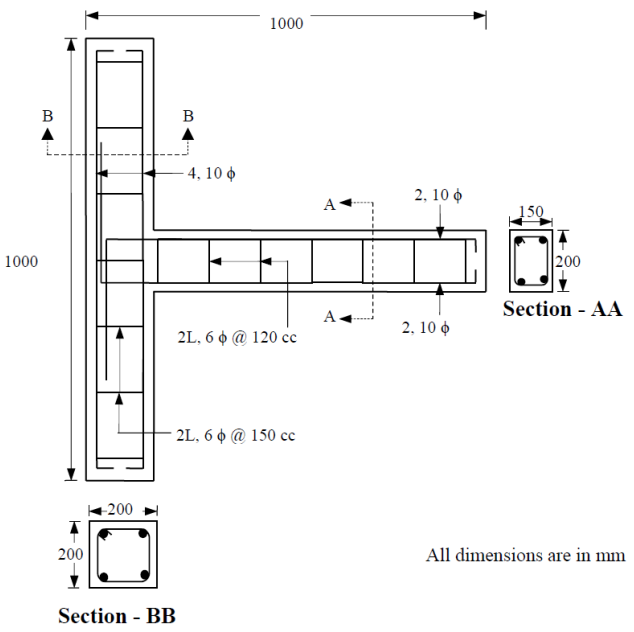

Fig. 1 Specimen details

Table 1 Properties of coarse and fine aggregate

Parameters	Coarse aggregate	Fine aggregate
Specific gravity	2.89	2.24
Bulk density (gm/cc)	1.54	1.23
Fineness modulus	7.05	3.15

Table 2 Properties of reinforcing steel

Nominal diameter (mm)	Unit weight (Kg/m)	Actual diameter (mm)	Yield strength (N/mm^2)	Ultimate strength (N/mm^2)	Modulus of elasticity (N/mm^2) $\times 10^5$
6	0.22	6.20	412.87	520.31	2.08
10	0.650	9.98	410.23	590.23	2.10

Table 3 Mix proportions

Mix	Fiber (%)	Fly ash (kg/m^3)	Na_2SiO_3 solution (kg/m^3)	NaOH solution (kg/m^3)	CA (kg/m^3)	FA (kg/m^3)	Water (kg/m^3)	SP (kg/m^3)
GPC	-	408	103	41	1252	600	14.5	10.2
SFRGPC1	0.25	408	103	41	1252	600	16.0	10.2
SFRGPC2	0.50	408	103	41	1252	600	16.0	14.5
SFRGPC3	0.75	408	103	41	1252	600	18.0	14.5
SFRGPC4	1.00	408	103	41	1252	600	18.0	16.0

are almost similar to that of conventional concrete beam column joints and the fibre addition enhanced the performance of beam column joints significantly (Ganesan *et al*. 2015, *Deepa et al.* 2016). In this study the performance of GPC beam column joints under reverse cyclic loading was investigated experimentally and analytically.

2. Experimental program

The experimental program involved the preparation and testing of plain and fiber reinforced GPC exterior beam column joints (GBJ) under reverse cyclic loading. The beam and column have cross sections 150 mm×200 mm and 200 mm×200 mm respectively. The longitudinal reinforcement in column consists of four 10 mm diameter high yield strength deformed (HYSD) bars. The top and bottom reinforcement of the beam consists of two 10mm diameter HYSD bars. The transverse ties in column and stirrups in beam consist of 6mm diameter bars. The overall dimensions and reinforcement details of the specimens are shown in Fig. 1. For fiber reinforced specimens the fiber volume fraction was varied to 1% at increments of 0.25%. Accordingly, the beam column joints were designated as GBJ1, GBJ2, GBJ3 and GBJ4 with fiber volume fraction 0.25%, 0.5%, 0.75% and 1% respectively.

2.1 Constituent materials

Ingredients of GPC were low calcium fly ash (Class F), coarse aggregate, fine aggregate, alkaline solution and super plasticiser. The physical and chemical tests results of fly ash conform to IS 3812 (Part I): 2003 specifications. Coarse aggregate (Crushed granite) of nominal size 20 mm and fine aggregate (river sand) conforming to Zone II of IS 383, 2016 were used for the study. The properties of coarse and fine aggregates used are given in Table 1. A mixture of sodium silicate solution and sodium hydroxide solution was chosen as the alkaline medium to activate the source material. Sodium silicate solution with SiO_2 to Na_2O ratio by mass of 2, i.e., Na_2O=14.7%, SiO_2 =29.4% and water=55.9% by mass was used. The sodium hydroxide solution was prepared by mixing sodium hydroxide pellets in water. Super plasticiser was also added to improve workability of concrete. Hooked end steel fibers with aspect ratio 60 (length 30 mm and diameter 0.5 mm) was used to prepare the steel fiber reinforced mix. High yield strength deformed (HYSD) bars having properties as given in Table 2 were used as reinforcement.

2.2 Mix design and specimen preparation

Since there is no codal recommendation available for the design of GPC mix, the mix design was done by performing various trials as per the guidelines proposed by Rangan (2006). For the trial mixes, alkaline liquid to fly ash ratio, fine aggregate to total aggregate ratio, molarity of NaOH solution, curing period and temperature, super plastisizer content and the extra water were considered as variables. Fiber reinforced GPC mixes (SFRGPC) were prepared by adding steel fibers to the GPC mix and varying super plasticiser dosage and water content to maintain a minimum slump value of 70 mm. Mix proportion for GPC and fiber reinforced GPC mixes are given in Table 3. The coarse aggregates and fine aggregate in saturated surface dry condition were mixed in laboratory pan mixer with fly ash for three minutes. Then the alkaline solutions, super plasticiser and extra water were added to the dry materials and mixed for four minutes. The workability of fresh concrete was determined by slump test and is given in Table 4. Standard cubes of size 150 mm, cylinders of 150 mm diameter and 300 mm height and prisms of size 100

Table 4 Fresh and hardened properties

Mix	GPC	SFRGPC1	SFRGPC2	SFRGPC3	SFRGPC4
Slump (mm)	103	95	80	75	73
Compacting factor	0.90	0.88	0.81	0.80	0.78
Compressive strength (N/mm^2)	37.00	37.40	38.35	39.00	39.10
Split tensile strength (N/mm^2)	3.56	3.80	4.20	4.50	4.70
Flexural strength (N/mm^2)	4.10	4.32	4.57	4.88	4.92
Modulus of elasticity (N/mm^2)	38148	39124	40116	40596	40725

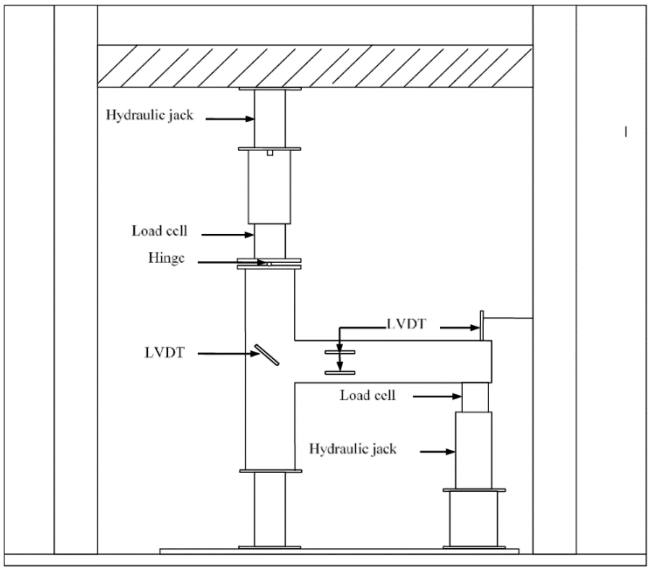

Fig. 2 Schematic diagram of test setup

mm×100 mm×500 mm were prepared to determine the hardened properties. All beam column joints were cast in moulds in layers. After one day of casting, the specimens along with moulds were oven cured at 60°C for 24 hours. Thereafter the specimens were removed from the oven and air-dried at room temperature for 24 hours before demoulding.

2.3 Testing of specimens

The specimens were tested in a loading frame. The top end of the column was provided with a hinged support, which was contrived by a steel ball placed between the grooves of two steel plates and its bottom end was simply supported. For making the column stable during testing, an axial compressive load of 20% of the axial load carrying capacity of the column was applied on the column by means of a hydraulic jack of capacity 1000 kN. Reverse cyclic loading was applied at the beam tip by using a hydraulic jack of 200 kN capacity. LVDT with a least count of 0.1 mm and 100 mm travel was placed at the beam tip to measure the deflections at beam tip. To measure the beam rotations one LVDT was placed at the level of top compression fiber and other was placed at the level of tension reinforcement, 25 mm from the bottom of the beam. The LVDT's had a gauge length of 50 mm with least count 0.001 mm. Schematic diagram of test set up and the test set

Fig. 3 Test setup

up fabricated in the lab are shown in Figs. 2 and 3 respectively. Each cycle of loading consists of a forward cycle and a backward cycle. For the first forward cycle, specimens were loaded to 1 kN and then unloaded to zero. For the backward cycle, the specimens were loaded to 1 kN in the reverse direction and unloaded to zero so that a full cycle of reverse cyclic loading can be obtained. For the second cycle, specimens were loaded to 2 kN, then unloaded to zero and in the backward cycle it was loaded in the opposite direction to 2 kN and unloaded to zero. This procedure was repeated for 3 kN, 4 kN etc. till the failure of the beam column joints. LVDT readings were taken for each cycle at intervals of 1 kN. Width of cracks was measured at regular intervals using a crack detection microscope with a least count of 0.02 mm up to 0.3 m.

2.4 Failure pattern

During testing the behavior of specimens were carefully observed. The specimens after test are shown in Fig. 4. As the load was gradually increased, the first crack was noticed in the beam portion near the joint in all the specimens these cracks propagated up to the beam top with further increase in loading and initial cracks started widening at the bottom. Finally the specimen failed by widening of cracks developed at the beam bottom. Majority of the cracks were centered in the beam portion near the joint. Fiber reinforced beam-column joints displayed closely spaced finer cracks. The increase in finer cracks was due to the presence of steel fibers embedded in concrete, which arrests widening of cracks. During the forward cycle, cracks appeared in the bottom portion of the beams and during backward cycle, cracks at bottom were closed and finer cracks formed at the top of the beam near the joint. After each cycle, new cracks were formed at different locations in the beam. Due to the presence of steel fibers, direction of crack propagation was not same. Hence it can be inferred that the steel fibers in concrete increased its resistance to crack propagation and widening. This led to the increase in the strength of beam column joints with the addition of fibers.

3. Results and discussions

3.1 Load-deflection behavior

(a) GBJ0

(b) GBJ1

(c) GBJ2

(d) GBJ3

(e) GBJ4

Fig. 4 Tested specimens

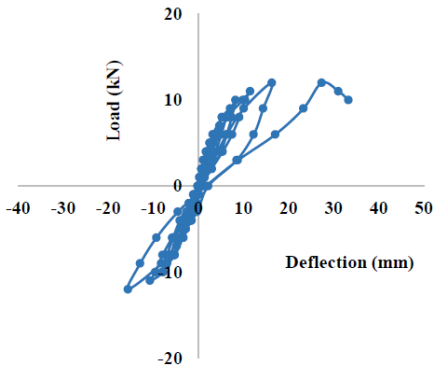

(a) GBJ0

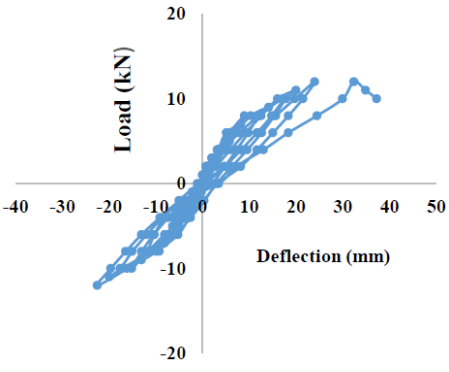

(b) GBJ1

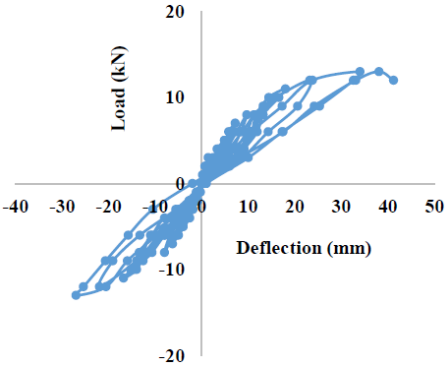

(c) GBJ2

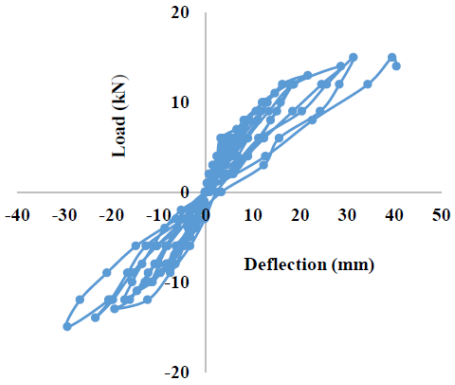

(d) GBJ3

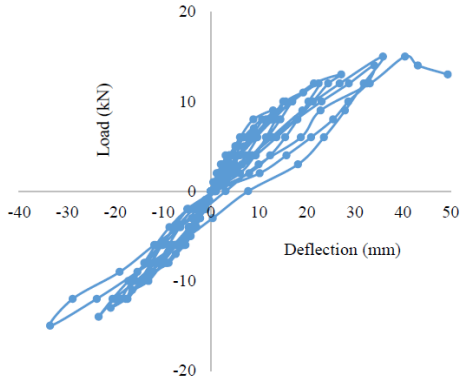

(e) GBJ4

Fig. 5 Load-deflection hysteresis plot

During testing, for every increment of load, the deflections at beam ends were recorded. From the recorded values, load deflection hysteresis curves were plotted and are shown in Fig. 5. The load deflection behavior of all GBJ specimens was almost similar in the initial cycles. For better understanding of the load deflection behavior, the load envelope curves for all the specimens were plotted and are shown in Fig. 6. Load envelope curves were drawn by plotting the peak loads and corresponding deflections in each cycle. From the graph, it can be observed that as the fiber content increased, deflection of the joint also increased and the joint with 1% fiber volume, GBJ4, has the maximum deflection than other GBJ specimens. The fibers resisted the formation of micro cracks as well as macro cracks. On development of micro cracks in the matrix, the steel fibers in the vicinity of such cracks arrested these cracks and prevented its further propagation. Due to this the load carrying capacity of the joints enhanced even under

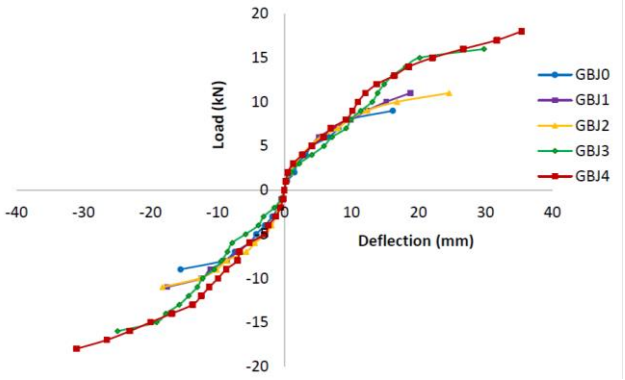

Fig. 6 Comparison of load- deflection envelope plots

Table 5 First crack load and ultimate load

Specimen	Cube strength (N/mm^2)	First crack load (kN)	Ultimate load (kN)	% increase in	
				First crack load	Ultimate Load
GBJ0	36.1	5.8	12	-	-
GBJ1	37.1	6.0	12	3.50	-
GBJ2	38.3	7.0	14	20.68	16.67
GBJ3	38.9	8.0	15	41.30	25.00
GBJ4	39.4	9.6	16	65.50	33.33

Table 6 Energy absorption capacity

Specimen	Deflection at ultimate load (mm)	Displacement ductility		Energy absorption capacity (kNmm)	
		Absolute (δ_u/δ_y)	Relative	Absolute	Relative
GBJ0	16.9	3.59	1.00	248.95	1.00
GBJ1	18.8	3.76	1.05	290.05	1.16
GBJ2	24.6	4.56	1.27	339.5	1.36
GBJ3	29.8	5.05	1.41	498.95	2.00
GBJ4	35.4	5.28	1.47	625.10	2.51

increased deflections.

3.2 First crack load and ultimate load

The first crack load was obtained from the load deflection envelope curves coinciding with the point at which the curve deviated from linearity and is given in Table 5. It is evident that the first crack load increased with increase in fiber content. This may be due the presence of steel fibers in concrete which increased the tensile strain carrying capacity of concrete. First crack load of GPC beam column joint with 1% fiber volume was 65% more than plain GPC beam column joint, which emphasizes the influence of fibers in concrete cracking.

Ultimate load is taken as the maximum load at which the joint failed, after producing excessive deflection. Table 5 shows the ultimate loads for specimens with varying fiber volume fractions. It can be observed from the table that ultimate load of the joints increased with increase in fiber volume. When the micro-cracks developed in the matrix, fibers intercepted the cracks and prevented its progression in that direction. This led the cracks in a deviated path for which more energy is required for propagating further and

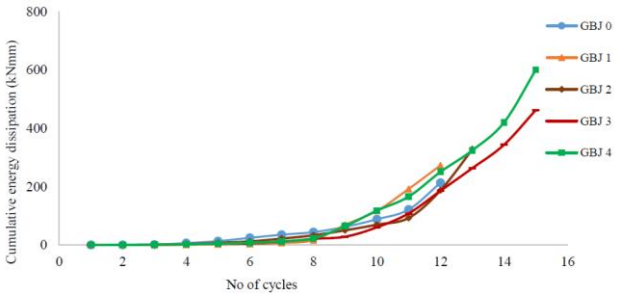

Fig. 7 Cumulative energy dissipation curve

improved its load carrying capacity. When subjected to cyclic loading the tip of the crack turned blunt on unloading. On reloading, more energy was required to reproduce the crack or to change its direction of propagation, which increased the ultimate load. Ultimate load was maximum for GPC joint with 1% fiber volume and it was 1.33 times more than that of plain GPC beam column joint.

3.3 Displacement ductility

The structures when subjected to repeated cycles of lateral loading should deform in a ductile manner. Ductility factor is the ratio of maximum deflection (δ_u) to the yield deflection (δ_y). The displacement ductility values of all the specimens are given in Table 6. From the table, it is evident that the ductility of the joints increased with increase in fiber content. It indicates that the presence of fibers in concrete improved the ductile behavior of the joints and made them resistant to cyclic loading. GBJ4 has the maximum ductility and it was 1.47 times more than that of GBJ0.

3.4 Energy absorption capacity

The energy absorption capacity is derived from the area enclosed by the load deflection envelope curve. The values of energy absorption capacity of all the specimens are given in Table 6. As per the table the energy absorption capacity increased consistently with the increase in fiber content and it is maximum for GBJ4, which is approximately 2.5 times higher than that of GBJ0.

3.5 Energy dissipation capacity

Energy-dissipation capacity is an important characteristic of the seismic performance of a structure. The structures can withstand severe earthquake motions only if they have sufficient capacity to dissipate seismic energy produced. The area under the hysteresis loop at given cycle represents the energy dissipated by the specimen in that cycle. The total energy dissipated by the specimen was calculated by summing up the energy dissipated in consecutive hysteresis loops throughout the test and is shown in Fig. 7. From the figure it can be inferred that fiber reinforced specimens have higher cumulative energy dissipation than plain specimens. The energy dissipation capacity of steel fiber reinforced specimens showed a

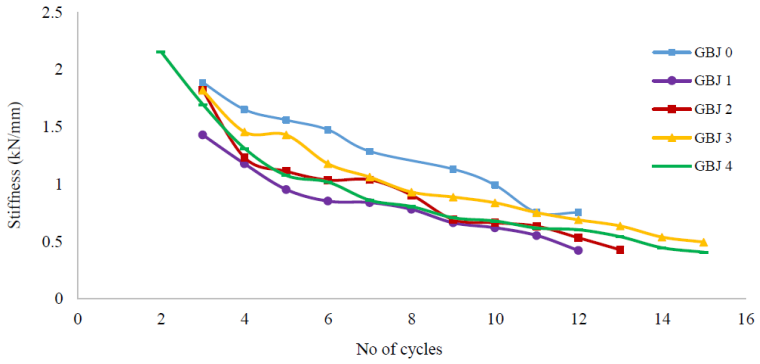

Fig. 8 Stiffness degradation curve

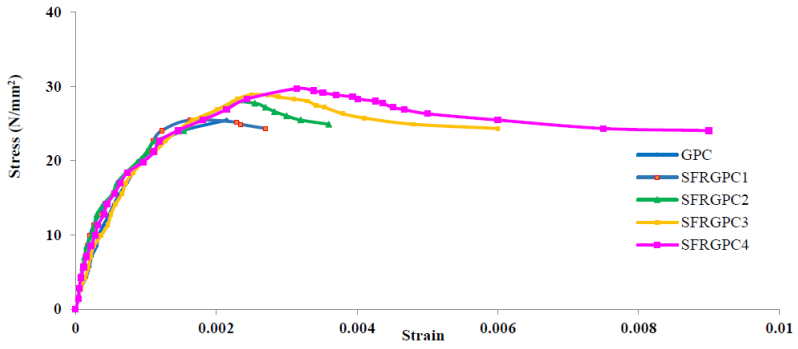

Fig. 9 Experimental stress strain curves

consistent increase with increase in fiber content.

3.6 Stiffness degradation

The stiffness of the joint gets reduced when it is subjected to cyclic or repeated loading. The materials like concrete and steel are subjected to loading, unloading and reloading cycles under cyclic loading. Due to this micro cracks may be formed in the joint and it may lead to fatigue failure. This increases the deformations inside the joints and can lead to reduction in joint stiffness. This degradation in stiffness can be assessed by computing secant stiffness. The slope of the line joining the points of maximum displacements in the forward and backward cycle gives the secant stiffness in that cycle. The stiffness degradation curve of all the specimens is shown in Fig. 8. As per the figure, GBJ0 has the lowest initial stiffness. For GBJ0, the curve has a steep slope, which indicates that rate of degradation of the stiffness is sudden. The rate of stiffness degradation decreased and the initial stiffness of the joints increased as the fiber content increased, GBJ4 has a flat slope which indicates that the rate of stiffness degradation is lowest for the specimen.

4. Finite element analysis of beam column joints

The non-linear response of reinforced concrete (RC) structures can be observed using the finite element method (FEM). Plain and fiber reinforced GPC beam column joints were modelled and analyzed using finite element software ANSYS.

4.1 Modeling

For modelling concrete Solid 65 element was used. It has eight nodes with three degrees of freedom per node i.e., translations in x, y, and z directions. This element is capable of plastic deformation, crushing and cracking in three orthogonal directions. Link 180 elements are used to model reinforcement. It has two nodes with three degrees of freedom per node i.e., translations in the nodal x, y and z directions. This element is also capable of plastic deformation. The joint was modelled using discrete reinforcement. Therefore, a value of zero was entered for all real constants which turned off the smeared reinforcement capability of the Solid 65 element. ANSYS requires material properties such as elastic modulus of concrete with varying fiber contents, density, uniaxial compressive strength, tensile strength, Poisson's ratio, opening and closing shear transfer coefficient as input details. Geopolymer concrete cubes cylinders for each fiber content were cast to determine the maximum uniaxial compresive strength, tensile strength and elastic modulus. Stress-strain curves obtained by testing cylinder specimens of 150 mm diameter and 300 mm height having fibre volume fractions 0.25% (SFRGPC1), 0.5% (SFRGPC2), 0.75% (SFRGPC3) and 1% (SFRGPC4) as shown in Fig. 9 was used for providing the multilinear isotropic stress-strain curve (Ganesan *et al.* 2015). The modulus of elasticity of all the mixes were calculated from the stress strain curve (initial tangent modulus), The material properties of 10 mm and 6 mm bars given in Table 2 was also given as input. The shear transfer coefficient for concrete represents the conditions of the crack face. This value can vary from 0.0 to 1.0 with 0.0

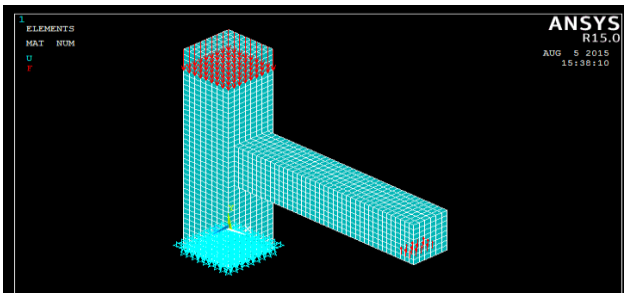

Fig. 10 Beam- column joint model

representing a smooth crack and 1.0 representing a rough crack. The value of shear transfer coefficient was taken as 0.2 for opening and 0.9 for closing as suggested in studies related to finite element modelling of reinforced concrete structures (Uma *et al.* 2012). The Poisson's ratio of geopolymer concrete is assumed as 0.2 (Ganesan *et al.* 2013). For providing perfect bond between materials the joint was modelled in such a way that the elements for concrete and steel shared the same nodes (Saravananand Kumaran 2011, Uma *et al.* 2012). Fig. 10 shows the model of the beam column joint created in ANSYS

4.2 Loading procedure

Non-linear static analysis was carried out. An axial load of 118 kN (20% of column capacity) was given at the top of column as axial force through nodes. The beam end was subjected to reverse cyclic loading. Each cycle of load was applied in sub steps through the nodes at the beam end. The cracks and crushing plot of the specimens before failure are Shown in Fig. 11. From the crack and crushing plot, it can be seen that cracks were mainly concentrated near the joint, which was similar to the behaviour observed during the testing.

5. Comparison of experimental and FEM results

5.1 Load-deflection behavior

The load deflection behavior obtained from the non-linear analysis is shown in Fig. 12. From the figure, it can be interpreted that the load hysteresis plot obtained from FEM was comparable with that obtained from the experimental study. From the crack and crushing plot, it can be seen that cracks were mainly concentrated near the joint, which was similar to the behaviour observed during the testing. For better comparison of results, the load envelope curve for the joint was plotted and compared with the experimental values. Fig. 13 shows the comparison load deflection envelope plot from experiment and from FEM analysis. From the figure it can be observed that the experimental curves were comparing satisfactorily with the curves obtained from FEM analysis.

5.2 Ultimate load and maximum deflection

Deflections obtained from numerical analysis were slightly less than that obtained from the experimental results whereas the ultimate load obtained from numerical analysis was slightly higher than that obtained from the experiment. The model in ANSYS is slightly stiffer than the actual specimens, since it uses ideal conditions for modelling. Bond slip and the contact between steel and concrete are not effectively considered in ANSYS modelling. The percentage difference between the results from the experiment and ANSYS are given in Table 7. From the table, it can be interpreted that the average variation in ultimate load and deflection at ultimate load between experiment and ANSYS are less than 15%. Therefore the model can be used for the analysis of geopolymer concrete beam column joint subjected to reverse cyclic loading.

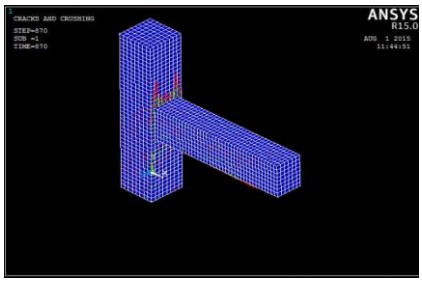

(a) Specimen GJ

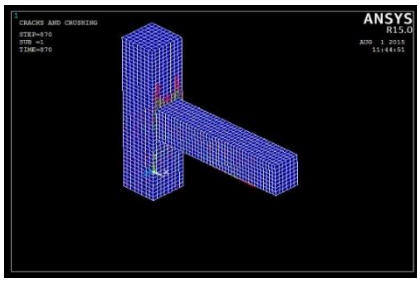

(b) Specimen GJ1

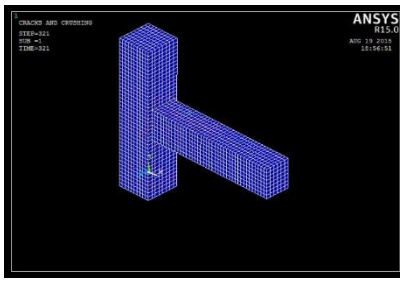

(c) Specimen GJ2

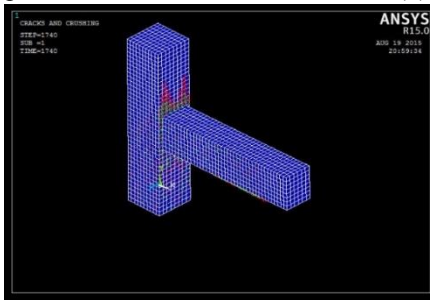

(d) Specimen GJ3

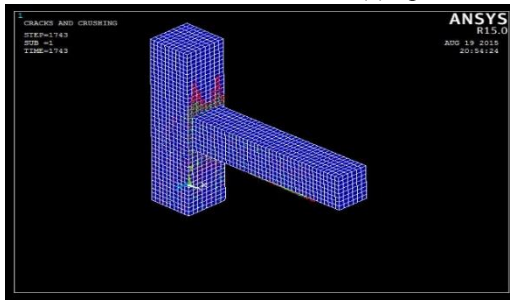

(e) Specimen GJ4

Fig. 11 Cracks and crushing of the specimens from ANSYS

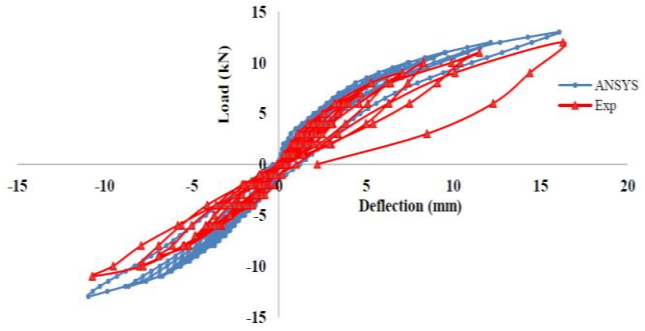

Fig. 12 Load-deflection hysteresis plot of GJ

Table 7 Comparison of results from experiment and ANSYS

Specimen	Ultimate load (kN)		% variation	Maximum Deflection (mm)		% variation
	Experiment	ANSYS		Experiment	ANSYS	
GBJ0	12	13	8.33	16.9	14.15	12.64
GBJ1	12	14	16.66	18.8	16.11	14.30
GBJ2	14	16	14.28	24.6	23.71	3.62
GBJ3	15	17	13.33	29.8	28.61	3.99
GBJ4	16	18	11.11	35.4	33.86	4.35
Average % variation			**13.02**		**7.78**	

6. Conclusions

The experimental and numerical study conducted lead to the following conclusions.

- Addition of fibers enhanced the performance of GPC beam column joints significantly.
- As the fiber content increased there is a marked improvement in first crack load and marginal to appreciable improvement in ultimate load. The above behavior happened up to an increase of 1% fiber content. However, fiber addition beyond 1% resulted in balling effect leading to workability problems. Hence fiber content up to 1% was considered in this study.
- Steel fiber reinforced specimens showed a consistent increase in the energy dissipation capacity with increase in fiber content. As the fiber content increased, the rate of stiffness degradation decreased and the initial stiffness of the joints increased.
- A numerical model of plain and fiber reinforced GPC beam column joint was developed using finite element software ANSYS. It can be used for the rational design of GPC beam column joints since the average percentage variation in ultimate load and maximum deflection between the experiment and FEM analysis was less than 15%.
- Test results of reverse cyclic loading on beam column joints revealed that the strength, ductility, energy absorption capacity and energy dissipation capacity could be enhanced by the use of SFRGPC. This indicated that it could be a suitable material for structures subjected to cyclic/seismic/impact/dynamic loading.

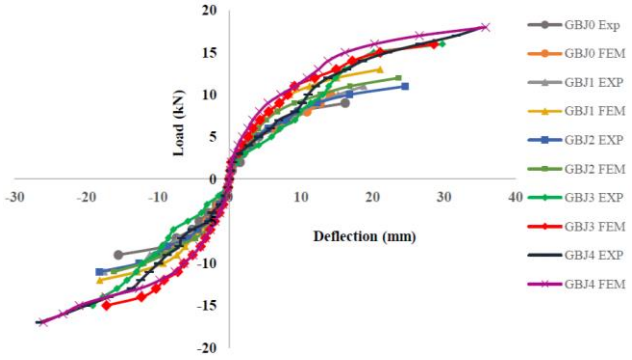

Fig. 13 Comparison of load-deflection envelope plots

Acknowledgements

The authors would like to thank the Kerala State Council for Science Technology and Environment (KSCSTE) for providing financial assistance to this work and the College of Engineering Trivandrum for supporting the work.

References

Bakhrev, T. (2006), "Geopolymeric materials prepared using Class F fly ash and elevated temperature curing", *Cement Concrete. Res.*, **35**(6), 1224-1232. https://doi.org/10.1016/j.cemconres.2004.06.031.

Dattreya, J.K., Rajamane, N.P., Sabhitha, D., Ambily, P.S. and Nataraja, M.C. (2011), "Flexural behavior of reinforced geopolymer concrete beams", *Int. J. Civil Struct. Eng.*, **2**(1), 138-159. https://doi.org/10.1109/ICEEOT.2016.7755347.

Duxson, P., Provis, J.L., Lukey, G.C. and Van Deventer, J.S. (2007), "The role of inorganic polymer technology in the development of green concrete", *Cement Concrete. Res.*, **37**, 1590-1597. https://doi.org/10.1016/j.cemconres.2007.08.018.

Ganesan, N., Abraham, R. and Raj, S.D. (2015), "Durability characteristics of steel fiber reinforced geopolymer concrete", *Constr. Build. Mater.*, **93**, 471-476. https://doi.org/10.1016/j.conbuildmat.2015.06.014.

Ganesan, N., Abraham, R. and Raj, S.D. (2015), "Effect of fibres on the stress-strain behaviour of geopolymer concrete", *Int. J. Earth Sci. Eng.*, **8**(4), 256-258.

Ganesan, N., Indira, P.V. and Sabeena, M.V. (2014), "Behavior of hybrid fiber reinforced concrete beam-column joints under reverse cyclic loads", *Mater. Des.*, **54**, 686-693. https://doi.org/10.1016/j.matdes.2013.08.076.

Ganesan, N., Indira, P.V. and Santhakumar, A. (2013), "Engineering properties of steel fibre reinforced geopolymer concrete", *Adv. Concrete Constr.*, **1**(4), 305-318. https://doi.org/10.12989/acc2013.1.4.305.

Hardjito, D. and Rangan, B.V. (2004), "On the development and properties of low calcium fly ash geopolymer concrete", *ACI Mater. J.*, **101**(6), 467-472.

IS 383-1970 (2016), Specifications for Coarse and Fine Aggregate from Natural Sources for Concrete-Code of Practice, 2nd Revision, BIS, New Delhi, India.

Jindal, B.B. (2018), "Feasibility study of ambient cured geopolymer concrete-A review", *Adv. Concrete Constr.*, **6**(4), 387-405. https://doi.org/10.12989/acc.2018.6.4.387.

Kurtoğlu, A.E., Alzeebaree, R., Aljumaili, O. and Niş, A. (2018), "Mechanical and durability Properties of fly ash and slag based

geopolymer concrete", *Adv. Concrete Constr.*, **6**(4), 345-362. https://doi.org/10.12989/acc.2018.6.4.345.

Lee, J.Y., Kim, J.Y. and Oh, G.J. (2009), "Strength deterioration of reinforced concrete beam -column joints subjected to cyclic loading", *Eng. Struct*., **31**(9), 2070-2085. https://doi.org/10.1016/j.engstruct.2009.03.009.

Raj, S.D., Ganesan, N., Abraham, R. and Raju, A. (2016), "Behaviour of geopolymer and conventional concrete beam column joints under reverse cyclic loading", *Adv. Concrete Constr.*, **4**(3), 161-172. http://dx.doi.org/10.12989/acc.2016.4.3.161.

Rangan, B. (2006), "Studies on low calcium fly ash based geopolymer concrete", *ICI J.*, 9-17.

Saravanan, J. and Kumaran, G. (2011), "Joint shear strength of FRP reinforced concrete beam-column joints", *Central Eur. J. Eng.*, **1**(1), 89-102. https://doi.org/10.2478/s13531-011-0009-6.

Sarker, P.K. (2009), "Analysis of geopolymer concrete columns", *Mater. Struct.*, **42**, 715-724. https://doi.org/10.1617/s11527-008-9415-5.

Sarker, P.K. (2011), "Bond strength of reinforcing steel embedded in fly ash-based geopolymer concrete", *Mater. Struct.*, **44**, 1021-1030. https://doi.org/10.1617/s11527-010-9683-8.

Shaikh, F.U. (2014), "Effect of alkali solutions on corrosion durability of geopolymer concrete", *Adv. Concrete Constr.*, **2**(2), 109-123. http://dx.doi.org/10.12989/acc.2014.2.2.109.

Sofi, M., Van Deventer, J.S.J., Mendis, P.A. and Lukey, G.C. (2007), "Engineering properties of inorganic polymer concretes", *Cement Concrete Res.*, **37**, 251-257. https://doi.org/10.1016/j.cemconres.2006.10.008.

Sujatha, T., Kannapiran, K. and Nagan, S. (2012), "Strength assessment of heat cured geopolymer concrete slender column", *Asian J. Civil Eng.*, **42**, 635-646.

Uma, K., Anuradha, R. and Venkatasubramani, R. (2012), "Experimental investigation and analytical modelling of reinforced geopolymer concrete beam", *Int. J. Civil Struct. Eng*., **2**, 817-827. https://doi.org/10.6088/ijcser.00202030010.

Wang, G.L., Dai, J.G. and Teng, J.G. (2012), "Shear strength model for RC beam-column joints under seismic loading", *Eng. Struct.*, **40**, 350-360. https://doi.org/10.1016/j.engstruct.2012.02.038.

CC